Interaction of NO with the Stoichiometric $RuO_2(110)$ Surface

Y. Wang, K. Jacobi,* and G. Ertl

Fritz-Haber-Institut der Max-Planck-Gesellschaft, Faradayweg 4-6, D-14195 Berlin, Germany

Received: June 30, 2003; In Final Form: September 12, 2003

The interaction of NO with the stoichiometric $RuO_2(110)$ surface, exposing coordinatively unsaturated Ru-cus and O-bridge atoms, was studied by thermal desorption spectroscopy (TDS) and high-resolution electron energy loss spectroscopy (HREELS). At low exposure ($\leq$0.5 L) and 85 K, NO is adsorbed on-top of Ru-cus with its molecular axis perpendicular to the surface for the first two-thirds of the monolayer and slightly bent when the final third is adsorbed. After saturation of this state, NO reacts with O-bridge in forming an NO_2-type surface species which decomposes again at 250 K. At higher exposure, a small amount of N_2O-cus is formed, presumably via an $(NO)_2$ dimer intermediate. In parallel, a low-temperature pathway for N_2 formation is observed, which leaves the surface instantaneously between 130 and 190 K.

1. Introduction

The interaction of NO with solid surfaces is of technological interest as the catalytic reduction of NO plays an important role in the control of air pollution. From a scientific point of view, the amphoteric nature of NO—due to the unpaired electron of the antibonding $2\pi^*$ molecular orbital—gives rise to a high complexity in adsorption on surfaces. The adsorption of NO on single-crystal metal surfaces has been extensively studied.[1] NO shows a tendency to undergo reactions on metal surfaces and besides NO, adsorbed species such as $(NO)_2$, N_2O, NO_2, as well as atomic N and O have been observed. Similar effects have been reported for metal oxide surfaces.[2] However, so far only a small number of studies have been performed on well-defined oxide surfaces.[3−5]

Recently, $RuO_2(110)$ surfaces have been prepared by exposing Ru(0001) to high doses of O_2 at elevated sample temperature.[6,7] The stoichiometric $RuO_2(110)$ surface (see a sketch in Figure 1) exposes coordinatively unsaturated atoms—Ru-cus and O-bridge—and has been found to exhibit high catalytic activity for CO oxidation.[7,8] Besides the fact that its structure is known, $RuO_2(110)$ is interesting because the chemically active surface atoms—Ru-cus and O-bridge—can be blocked or removed separately, enabling straightforward identification of the actual sites of reactivity.

In the present work we study the interaction of NO with the stoichiometric $RuO_2(110)$ surface by using thermal desorption spectroscopy (TDS) and high-resolution electron energy loss spectroscopy (HREELS). Three types of surface species are identified: chemisorbed NO on-top of Ru-cus, NO_2 from the interaction of NO with O-bridge, and N_2O formed via an $(NO)_2$ intermediate. In addition, a low-temperature pathway forming N_2 is detected, i.e., even a reduction of NO.

2. Experimental Section

The experiments were performed in an ultrahigh vacuum (UHV) apparatus consisting of two chambers separated by a valve. The base pressure was 2×10^{-11} mbar. The upper chamber was used for sample preparation and contained facilities for TDS, low-energy electron diffraction (LEED), gas dosing, and surface cleaning by Ar ion sputtering. The lower chamber housed a HREEL spectrometer of commercial Ibach design (Delta 0.5, SPECS, Germany). HREEL spectra were taken in specular geometry at an angle of incidence of 55° with respect to the surface normal. The primary electron energy was set to 3 eV and the energy resolution was better than 2.5 meV.

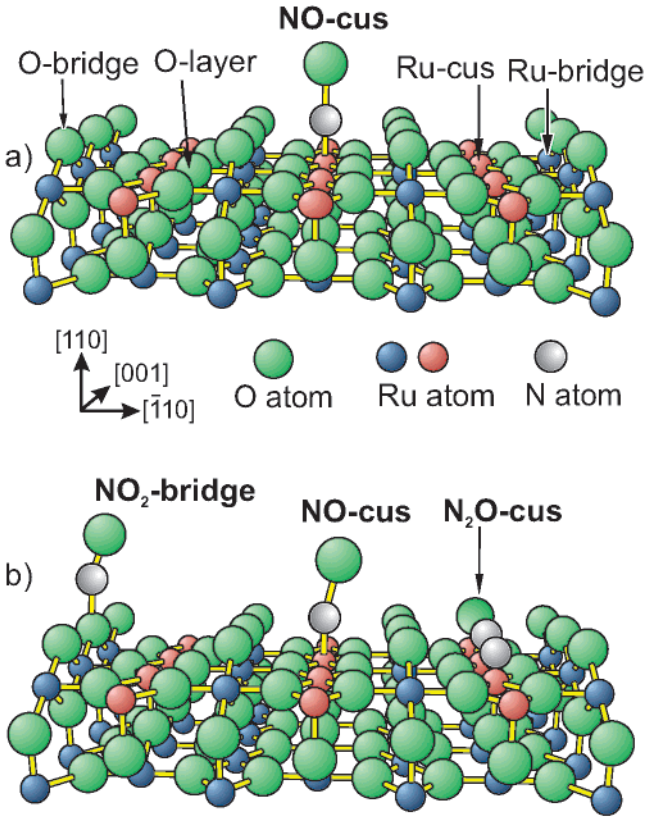

Figure 1. Ball-and-stick model of the stoichiometric $RuO_2(110)$ surface in perspective view. The NO-cus, NO_2-bridge, and N_2O-cus surface groups are also sketched.

* Corresponding author. Phone: ++49 30 8413 5201. Fax: ++49 30 8413 5106-3155. E-mail: jacobi@fhi-berlin.mpg.de.

10.1021/jp0308108 CCC: $25.00
Published on Web 11/20/2003

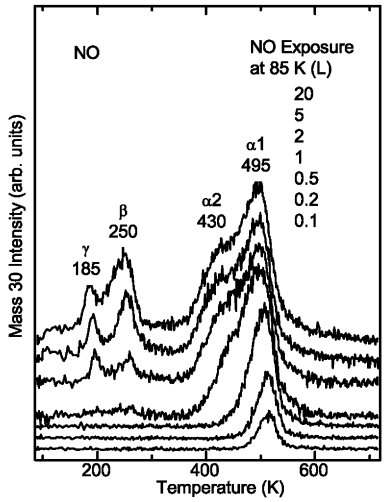

Figure 2. NO (mass 30) TD spectra for various NO exposures at 85 K on the stoichiometric $RuO_2(110)$ surface. The heating rate was 3 K/s.

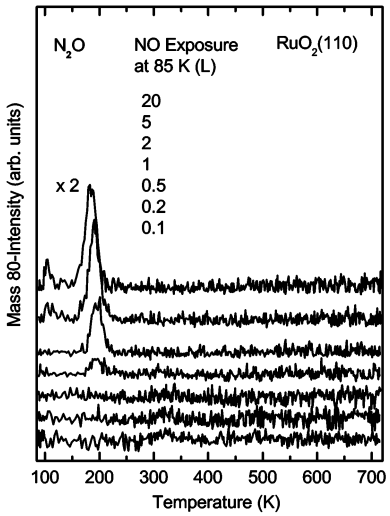

Figure 3. N_2O (mass 44) TD spectra for various NO exposures at 85 K on the stoichiometric $RuO_2(110)$ surface. The heating rate was 3 K/s. The factor 2 is with respect to the intensities in Figures 2 and 4.

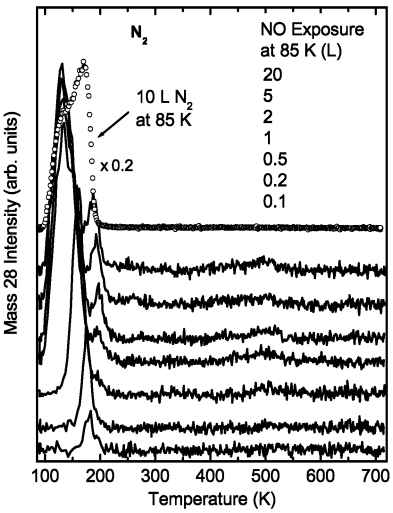

Figure 4. N_2 (mass 28) TD spectra for various NO exposures at 85 K on the stoichiometric $RuO_2(110)$ surface. The heating rate was 3 K/s.

3. Results

3.1. Thermal Desorption Spectra. The TD spectra of NO (mass 30), recorded for increasing NO exposure at 85 K, are presented in Figure 2. At low exposure only one desorption peak at around 510 K is observed. This state is saturated after exposing the sample to 0.5−1.0 L NO. The desorption peak shifts slightly downward by 15 K. With increasing NO exposure, new features evolve at lower temperatures. At an exposure of about 20 L, saturation is reached and the TD spectrum exhibits the following four desorption peaks: α_1-NO (495 K), α_2-NO (430 K), β-NO (250 K), and γ-NO (185 K).

To check for dissociation of NO, we performed TDS measurements at mass 28 for N_2, 44 for N_2O, and 46 for NO_2. Desorption of NO_2 was not observed. The TD spectra for N_2O and N_2 are presented in Figures 3 and 4, respectively. The spectra of mass 44 are representative for N_2O rather than CO_2, because the vibrational mode at 291 meV, characteristic for CO_2 adsorbed on $RuO_2(110)$,[9,10] was not observed in the HREEL spectra shown below. Associative desorption of atomic nitrogen—which is expected to occur at higher temperatures in analogy to atomic O—is not observed, which means that there is no evidence for dissociation of NO into atomic N and O.

Interestingly, we find additional, rather strong desorption of N_2 whose peak maximum shifts from 180 to 130 K with increasing exposure. In Figure 4 we have added a TD spectrum of N_2 following exposure of the stoichiometric surface to 10 L of N_2 at 85 K. This spectrum is due to N_2 chemisorbed at Ru-cus and differs from the spectra measured after NO interaction. Therefore, we believe that the N_2, observed already at small exposures to some degree and to grow with exposure while the peak maximum shifts down to 130 K, is a molecular reaction product from thermal decomposition of N_2O on $RuO_2(110)$ according to

$$NO + NO \rightarrow (NO)_2 \rightarrow N_2O + O_{ad} \rightarrow N_2\uparrow + 2O_{ad} \quad (1)$$

When increasing the surface temperature during TDS, reaction 1 could not be separated into single steps, but leads immediately to the end product N_2 which desorbs. The main proof for this interpretation originates from the HREELS results presented below which do not show a strong ν(N−N) mode indicative of an N_2-containing stable intermediate, although there is clear evidence for N_2 desorption in TDS.

Only for exposures ≥1 L, also an N_2O intermediate is observed in TDS besides the N_2 end product (Figure 3). The N_2O desorption peak exhibits a slight shift from 195 to 185 K

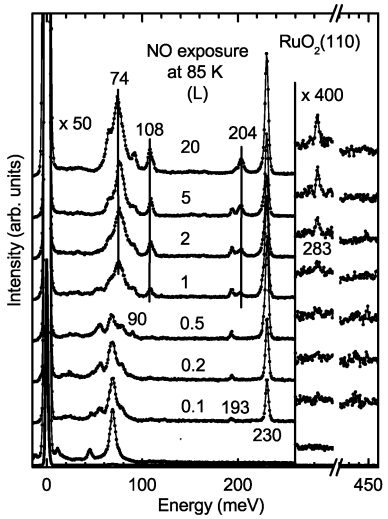

Figure 5. HREEL spectra for various NO exposures at 85 K on the stoichiometric $RuO_2(110)$ surface. All spectra were recorded at 85 K in specular geometry with an incidence angle of 55° with respect to the surface normal and with a primary energy of 3 eV. The factors ×50 and ×400 are relative to the elastic intensity.

TABLE 1: Activation Energies for Formation, Desorption, or Decomposition of N_2, NO, N_2O, and NO_2 Following Exposure of the $RuO_2(110)$ Surface to NO

	N_2 formation	N_2O desorption	NO_2 decomposition	NO desorption	
				α2	α1
E (kJ/mol)	33	47	64	112	129

TABLE 2: Vibrational Energies [meV] and Mode Assignments for Chemisorbed NO, Reacted N_2O, $N^{16}O_2$, and $N^{18}O^{16}O$ on the $RuO_2(110)$ Surface (The vibrational modes are denominated as: *ν*, stretching mode; *δ*, bending mode)

modes	NO	N_2O	$N^{16}O_2$	$N^{18}O^{16}O$
ν(Ru−NO_x)	41		74	72.2
δ(NO_x)	90		108	106.5
ν(N−O)	230		204	204
ν(N−N)		283		

with increasing exposures. The accompanying NO desorption peaks (γ-NO) and N_2 (in Figure 4 at the same temperature) are attributed to cracking products of N_2O in the mass spectrometer.

So, for NO exposure ≥1 L, obviously two channels open up with annealing. Besides desorption of the end product N_2 of the reaction sequence (eq 1), a small amount of the presumed reaction intermediate N_2O is found by TDS as well as by HREELS, the latter shown below. The desorption of N_2 is of first order since this species is likely to be generated by decomposition of N_2O. Assuming a preexponential factor of 10^{13} s^{-1} in the Redhead formula,[11] the activation energy for the associated process was derived and is given in Table 1. The other NO desorption peaks (α1, α2, β) will be assigned with the help of the HREELS data presented in the following.

3.2. HREEL Spectra. To characterize the adsorbed species as well as the anticipated reaction intermediates, we recorded vibrational spectra by means of HREELS. A series of spectra, taken at 85 K as a function of NO exposure, is presented in Figure 5. The stoichiometric $RuO_2(110)$ surface exhibits vibrational modes at 12, 45, and 69 meV (see the bottom spectrum), among them the dominant peak at 69 meV from the normal stretching mode of O-bridge,[12] and the losses at 12 and 45 meV presumably from phonons. The observed energies and mode assignments for the adsorbed species are summarized in Table 2 and will be discussed in the following.

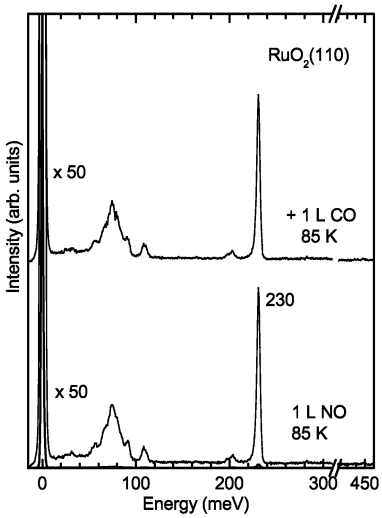

Figure 6. HREEL spectra recorded after the stoichiometric $RuO_2(110)$ surface was exposed to (a) 1 L of NO at 85 K and then (b) 1 L of CO at 85 K. Parameters as for Figure 5.

3.2.1. Adsorption of NO at 85 K: Chemisorbed NO-cus. After exposure to 0.1 L of NO at 85 K, a pronounced peak at 230 meV appears that is assigned to the ν(N−O) stretching mode in analogy to the corresponding gas-phase value of 233 meV.[13] It saturates in intensity at about 0.5 L. The high energy of the ν(N−O) mode and the absence of a bending mode for exposure <0.5 L suggest a linear on-top configuration of NO with its molecular axis perpendicular to the surface. The weak feature at 193 meV observed for all spectra in Figure 5 may be attributed to NO bonded at domain boundaries, because it decreases in intensity for better prepared surfaces. Other weak features observed at 58, 78, 437, and 448 meV increase with collection time of the HREEL spectra and decrease with NO exposure and are therefore associated with a H_2O-like species formed through dissociative adsorption of H_2 at O-bridge.[14] From our recent measurements it is known that adsorption of hydrogen from the residual gas cannot be completely suppressed for the reactive $RuO_2(110)$ surface even at a background pressure of 2×10^{-11} mbar.

To identify the adsorption site of this species, the following experiment was conducted. The sample was exposed to 1 L of NO at 85 K and subsequently to 1 L of CO. As shown in Figure 6, the spectrum remains unaffected by CO exposure. The expected ν(Ru−CO) and ν(C−O) modes at 38 and 260 meV, respectively, characteristic for CO bonded to Ru-cus[7,8] are not observed. This means that CO adsorption on Ru-cus sites is inhibited by NO preadsorption. For the stoichiometric surface without any preadsorbate, we conclude therefore that NO is adsorbed on Ru-cus and call it NO-cus (see Figure 1). A normal orientation of the NO axis is suggested by the geometry of the Ru-cus dangling bond stretching perpendicularly out off the surface.[6] Interestingly, for exposure ≥ 0.5 L, a small peak is observed at 90 meV assigned to an NO bending mode. This is somewhat surprising as there is no steric reason for NO-cus to bend its molecular axis out of the surface normal since the distance of Ru-cus amounts to 3.18 Å which is much larger than an expected minimal NO−NO distance. From the same exposure range, the α1 and α2 TDS peaks are identified as due to NO-cus.

3.2.2. Adsorption of NO at 85 K: Formation of NO_2-Bridge. When the exposure to NO is increased to ≥1 L and the β and δ peaks are observed in TDS, new peaks at 75, 108, and 204 meV evolve (see Figure 5). These peaks grow with NO

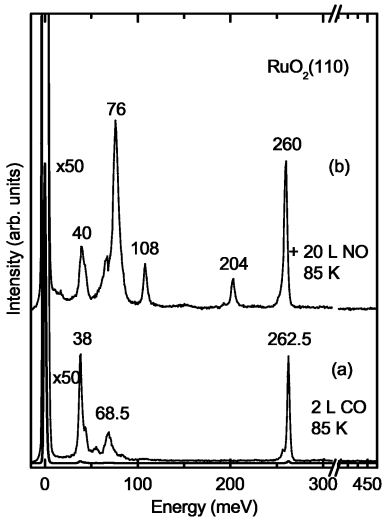

Figure 7. HREEL spectra recorded after the stoichiometric RuO_2(110) surface was exposed to (a) 2 L of CO at 85 K and then (b) 20 L of NO at 85 K. Parameters as for Figure 5.

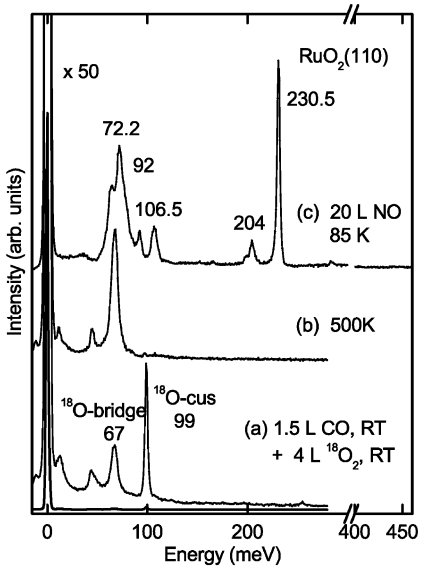

Figure 8. HREEL spectra recorded after the stoichiometric RuO_2(110) surface was exposed to (a) 1.5 L of CO at 300 K and then 4 L of $^{18}O_2$ at 300 K; (b) sample a was annealed to 500 K; (c) after a further exposure of sample b to 20 L of NO at 85 K. Parameters as for Figure 5.

exposure, while the NO-cus-induced losses remain unchanged. Since the assignment of the new losses is not straightforward, the following experiment was performed. First, the sample was preexposed to 2 L of CO at 85 K in order to block the Ru-cus sites. In curve a of Figure 7, one recognizes the ν(Ru−CO) and ν(C−O) modes of CO-cus at 38 and 262 meV known for CO molecules in terminal configuration on Ru-cus.[7] Then, this surface was exposed to 20 L of NO. In curve b of Figure 7 no NO-cus induced modes are observed, whereas the losses at 76, 108, and 204 meV are observed with strong intensity. The slight shift in energy of the loss at 74 meV in Figure 5 to 76 meV in curve b of Figure 7 as well as of the CO-induced losses at 38 and 262.5 meV in curve a to 40 and 260 meV in curve b of Figure 7 can be explained in terms of interaction between coadsorbed NO and CO. The experiment of Figure 7 reveals that here NO chemisorbs at O-bridge. The following isotope substitution experiment provides further support for this conclusion.

First, a reduced RuO_2(110) surface was prepared by exposing the surface to 1.5 L of CO at room temperature so that O-bridge was removed via the reaction with CO to CO_2 which leaves the surface immediately.[8] Then, by exposing 4 L of $^{18}O_2$, the surface was completely restored and transformed into the oxygen-rich state as becomes evident from change of the stretching mode energies from 69 to 67 meV for ^{18}O-bridge and from 103 to 99 meV for ^{18}O-cus (curve a in Figure 8), corresponding to an isotope shift of 1.04.[8] After annealing to 500 K, ^{18}O-cus was completely desorbed, so that a stoichiometric RuO_2(110) surface with ^{18}O-bridge was left (curve b in Figure 8). This surface was further exposed to 20 L of NO at 85 K. The frequencies of the NO-cus-related modes (92 and 230.5 meV) do not exhibit any isotope shift, whereas the losses under discussion, formerly at 74 and 108 meV, shift to lower frequencies, as expected for a formation of ^{16}ON^{18}O on Ru-bridge via bonding of N^{16}O to ^{18}O-bridge. Interestingly, the loss at 204 meV shows no isotopic shift, which will be rationalized below. We conclude that the losses at 74, 108, and 204 meV are due to a nitrogen dioxide surface group, sketched in Figure 1b, which we call NO_2-bridge.

It is known that there are four main types of coordination for NO_2 at a surface: (a) N-coordination (N-bonded), (b) O-coordination (O-bonded), (c) N,O-coordination (side-on bonded), and (d) O,O-coordination (O,O-bonded).[15] An O-bonded configuration is expected for NO_2 formed via bonding of NO with its N-end to O-bridge. Thus, the observed peaks at 74, 108, and 204 meV can be assigned to the frustrated translation perpendicular to the surface ν(Ru−ONO′), the bending mode δ(ONO′), and the stretching mode ν(N−O′) (O′ being the outer oxygen atom), respectively. This assignment is supported by the above isotope substitution experiment (Figure 8). An isotopic shift, predicted within the harmonic oscillator approximation, is observed for the ν(Ru−^{18}ON^{16}O′) and δ(^{18}ON^{16}O′) modes, whereas the ν(N−^{16}O′) mode is not shifted. As O-bridge is basically sp^2 hybridized, exhibiting one dangling bond perpendicular to the surface, we assume that the O-bridge-NO′ bond is perpendicular to the surface and the outer NO′ bond is bent.

3.2.3. Adsorption of NO at 85 K: Formation of N_2O. For NO exposure ≥1 L, the spectra in Figure 5 display an additional weak loss at 283 meV which gains in intensity with increasing NO exposures. Since for the same exposure a N_2O signal is observed in TDS, we attribute this mode to the N−N stretching mode ν(N−N) characteristic for N_2O. This assignment is further supported by the following experiment. The stoichiometric RuO_2(110) surface was exposed to 10 L of N_2 at 85 K, and the corresponding HREEL spectrum is shown in Figure 9. The N−N stretching mode ν(N−N) of N_2 is found to be 287 meV, i.e., near to the gas-phase value of 289 meV. Both the stretching mode energy and the low desorption temperature (see Figure 4) indicate that N_2 is weakly chemisorbed. The weak intensity of ν(N−N) indicates that N_2 may be adsorbed parallel to the surface so that it is excited only through impact scattering. Other peaks observed at 25, 57, 108, and 226 meV are due to H_2O-like species formed through the interaction of H_2 from the residual gas with O-bridge.[14] We exclude therefore an assignment of the loss at 283 meV as due to N_2. Again, the weakness of the ν(N−N) mode and the absence of an additional ν(N−O) mode suggest that N_2O lies horizontally on the surface (see Figure 1b).

For the formation of N_2O on metal surfaces, two reaction pathways have been suggested.[1] The first reaction pathway was

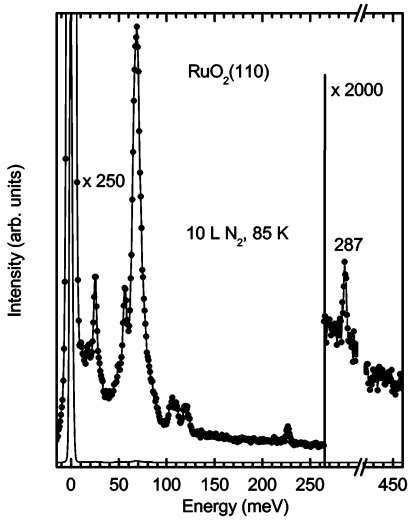

Figure 9. HREEL spectrum for an exposure of 10 L of N_2 on the stoichiometric $RuO_2(110)$ surface at 85 K. Parameters as for Figure 5.

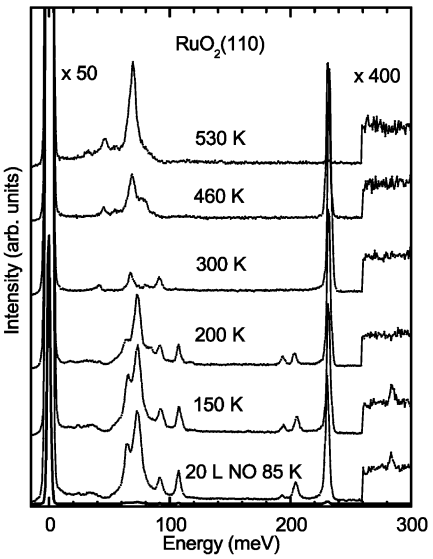

Figure 10. HREEL spectra for an exposure of 20 L of NO on the stoichiometric $RuO_2(110)$ surface. After exposure at 85 K, the sample was subsequently annealed to the indicated temperatures. Parameters as for Figure 5.

already noted in eq 1. The second is as follows:

$$2NO \rightarrow 2NO_{ad} \rightarrow NO_{ad} + N_{ad} + O_{ad} \rightarrow N_2O_{ad} + O_{ad} \quad (2)$$

For this pathway (eq 2), a necessary condition is the presence of atomic nitrogen on the surface from a concomitant dissociation of NO. The earlier pathway (eq 1) is a nondissociative reaction sequence with a $(NO)_2$ dimer as intermediate. The fact that the atomic nitrogen was not found on the $RuO_2(110)$ surface favors the earlier pathway (eq 1). This reaction favorably proceeds at high NO coverage when dimer formation may be initialized most easily.

Although N_2O formation is accompanied by split-off of atomic oxygen, the corresponding ν(Ru−O) vibrational mode at about 103 meV was not detected (Figure 5). Its invisibility might be caused by a strong screening through coadsorbed NO and N_2O as reported similarly for Ru(0001).[16]

3.2.4. HREELS after Annealing to Higher Temperatures. The stoichiometric $RuO_2(110)$ surface was exposed to 20 L of NO at 85 K, and subsequently annealed to the temperatures indicated in Figure 10. The respective HREEL spectra were then recorded again at 85 K. After annealing to 150 K the spectrum remains nearly unchanged, only the integrated intensity of the ν(N−N) mode at 283 meV due to N_2O is increased and some N_2O has been decomposed leading to N_2 desorption (Figure 4). This means that a further formation of N_2O occurs with annealing. Upon heating to 200 K, N_2O is no longer observed, in agreement with the N_2O desorption at 185 K.

After annealing to 200 K, the NO_2-induced losses at 74, 108, and 204 meV lose slightly in intensity and disappear entirely during annealing to 300 K. Because NO_2 desorption is not observed in the TD spectra, the disappearance of NO_2-induced peaks can only be attributed to NO_2 decomposition into O-bridge and NO. The latter leaves the surface to some degree giving rise to the β-NO desorption peak at around 245 K. From TDS, a decomposition energy or NO desorption energy of 64 kJ/mol was derived (Table 1). The remaining part fills up the empty Ru-cus sites as indicated by the increase of the ν(N−O) intensity by about 50%. Ru-cus sites are found empty from the desorption of N_2O and N_2. So, at 300 K only NO-cus is present on the surface and its δ(NO) and ν(N−O) modes are observed at 90 and 230 meV. Now a peak at 41 meV has evolved out of the broader background observed for these energies at lower annealing temperatures. This mode can be assigned to the stretching mode of NO against Ru-cus.

By heating to 460 K, the α_2-NO is released into vacuum. The NO bending mode at 90 meV disappeared, while the ν(N−O) mode decreased in intensity by 30%. This indicates desorption of bent NO or a partial desorption of NO and a concomitant conversion of the remaining bent NO-cus into linear NO-cus. The α_2-NO state is therefore associated with that part of NO-cus which leads to a bending of NO-cus. After further annealing to 530 K, the linear NO-cus, corresponding to α_1-NO, desorbed completely. The spectrum displays again the dominant peak at 69 meV characteristic for the stoichiometric $RuO_2(110)$ surface.

4. Discussion

The TD and HREEL spectra indicate that the interaction of NO with the $RuO_2(110)$ surface is quite complex and depends strongly on coverage and temperature. At low coverage (NO exposure < 0.5 L, α_1 state) NO molecules interact solely with Ru-cus atoms leading to chemisorption of NO-cus. NO-cus is more strongly bonded than any other NO-derived molecule discussed below (see Table 1). Guided by the work on metal surfaces we conclude that NO bonds with its nitrogen end to Ru-cus. Since Ru−cus exhibits a kind of dangling bond normal to the surface[6] it is reasonable to assume that NO stands upright on the surface. This is supported by the missing bending mode.

Interestingly, an NO bending mode is observed when the final third of the NO-cus ML (the α_2 state, see also Table 1) is adsorbed which is more weakly bonded than the first two-thirds (α_1 state). Normally the Pauli repulsion between neighboring NO molecules is invoked to account for the conversion from linear to bent NO. On the other hand, the separation of the Ru-cus sites is so large (3.18 Å) that there is no need for a bending of NO-cus. So, considering NO adsorption on Ru-cus under a pure steric aspect does not explain the NO bending. Since we do not envisage an additional site for NO-cus, we are led to infer an electronic effect for an explanation. A decisive conclusion might be obtained by an electronic structure calculation.

The ν(N−O) mode is blue-shifted by 6 meV with respect to the value found for NO adsorbed on Ru(0001).[17] This points to

a reduction of electron back-donation into the NO $2\pi^*$ antibonding orbital in the case of RuO_2. An analogous behavior has been reported for NO adsorbed on Ru(0001), pre-covered by oxygen.[16] In this case the preadsorbed oxygen reduces the local electron density at the Fermi level of the Ru surface atoms and reduces thereby the ability of the surface for back-donation of electrons.

Besides NO-cus, the second important product of the NO interaction with the RuO_2 surface is an NO_2-type surface species. We have demonstrated that it arises from interaction of NO with O-bridge. However, it cannot be simply interpreted as NO chemisorbed at O-bridge because the resulting vibrational spectrum can only be rationalized in terms of NO_2. Nevertheless, during annealing NO_2 breaks apart at the same bond between O-bridge and N which is formed during chemisorption. A similar formation of a surface group including O-bridge was observed recently in the case of H_2 adsorption: A H_2O-like surface molecule is formed when H_2 dissociates at O-bridge.[14] A similar chemisorption of NO in forming NO_2 on top of oxygen has been observed already for some metal-oxide surfaces, e.g., on BaO[18] and CeO.[2]

Nitrito transition-metal complexes show a stretching mode ν(N−O′) at 173−184 meV[13] which is lower than the 204 meV observed here. This can be explained in terms of the chemical shift effect due to the coexistence of electronegative O-bridge atoms, which result in reduced electron back-donation into the σ_x^* antibonding orbital of adsorbed NO_2 and consequently a stiffening of the intramolecular N−O′ bond. A similar behavior has been reported for NO adsorption on a Ru(0001) surface, where the ν(N−O) mode of NO bonded on 2-fold bridge site shifted from 186 to 197 meV after the surface was modified by oxygen.[16] Note that here a ν(N−O) mode is not found, since a weak dynamic dipole moment and some shielding through the NO′ end seem to prevent its detection.

While the dissociation of NO into atomic N and O does not take place on RuO_2(110), a low-temperature pathway leading to the formation of N_2 is observed. This is the third product from the interaction of NO with the RuO_2 surface which is, however, not stable at the surface at the formation temperature of 130 to 190 K. Also here, for the formation of N_2 during warming the surface to 200 K, an $(NO)_2$ intermediate has to be taken into consideration (see eq 1). From the smallest exposure on, N_2 desorption is observed shifting from 190 to 130 K (see Figure 4). A reaction is taking place whose main product, N_2, leaves the surface instantaneously. The other product, O-cus, expected to be left at the surface, could not be detected. Either it is shielded by the remaining NO or it may be incorporated into the bulk in course of the surface reaction which presumably activates substrate bonds. No reaction intermediate was frozen in under these conditions. We have no explanation for this reaction other than the presumption that it proceeds via $(NO)_2$-dimer and N_2O formation (reaction).

Now we turn to N_2O which is a fourth (but minor) product formed by interaction of NO with RuO_2(110) at an NO exposure ≥1 L. Its formation is less well understood. It desorbs at 190 K, giving rise to N_2O as well as N_2 and NO signals from the cracking process in the mass spectrometer (γ-NO in Figure 2). In eqs 1 and 2 we have already sketched the two pathways which are discussed for the formation of N_2O. Our conclusion is that the pathway of eq 1, which is based on the formation of an $(NO)_2$ dimer, is operative. The existence of NO dimers in condensed phases[19] and even in the gas phase[20] is well-known. The formation of $(NO)_2$ dimers has also been observed on some metal[1] and postulated on a MgO surface as intermediate for

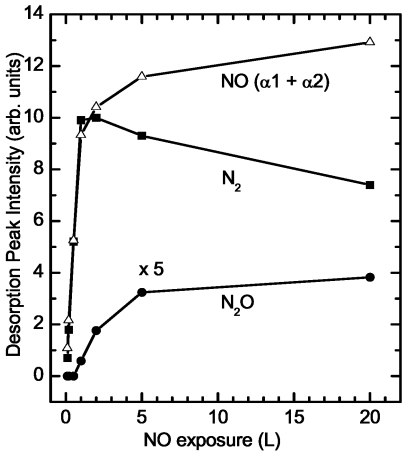

Figure 11. Integrated intensities of the respective desorption peaks for NO ($\alpha1 + \alpha2$), N_2O, and N_2 as a function of NO exposure.

N_2O formation.[5] NO is able to dimerize by forming a weak N−N bond involving mainly the unpaired 2π valence orbitals of the monomer. It is not clear, at the moment, how a dimer can be formed from NO-cus in our case. The involvement of NO-cus, on the other hand, follows from the observation that there are empty Ru-cus sites left at the surface after desorption of N_2O and of N_2. This was demonstrated by the fact that the coverage of NO-cus is increased by NO from the decomposing NO_2-bridge. Finally we have to admit that further details of the reaction from $(NO)_2$ to N_2O are unclear. Normally it is assumed that the dimer is parallel to the surface as to allow to split-off O through interaction with the substrate. Such a geometry is hard to imagine for RuO_2(110).

To estimate the relative amounts of the different products, a quantitative analysis was performed by integrating the respective desorption peaks, taking into account the ionization gauge sensitivity factor for each species. Figure 11 shows the resulting desorption yields for NO, N_2O, and N_2 as a function of NO exposure. The NO yield is calculated as the sum of the α_1 and the α_2 peak due to NO desorption from Ru-cus. At first, the yields of NO and N_2 increase rapidly, whereas the signal of N_2O is not detected. At an exposure of about 1 L the amount of N_2 is saturated at a level corresponding to decomposition of about 50% of the NO-cus molecules. As the exposure is further increased, the signal of NO increases further and that for N_2O evolves, whereas that of N_2 decreases slowly. At saturation coverage, the ratio of the intensities of NO, N_2O, and N_2 is evaluated as 13:0.8:7.4. This shows that a large fraction of N_2-containing species (90%) decomposes and only a minor fraction desorbs as N_2O, consistent with the finding that N_2 formation has a lower activation energy than N_2O desorption (see Table 1). We also compared the amount of the decomposed N_2 with that from a saturated N_2 layer (or better row) on Ru-cus: The decomposed N_2 amounts to 1/4 of the full N_2-cus row, i.e., half a NO-cus row reacts to N_2O. This amount compares reasonably well with the 1/3 empty Ru-cus sites estimated from refilling with NO from NO_2 decomposition. Half a NO-cus row means 25% of a full NO coverage (from NO-cus as well as NO_2-bridge).

The absence of NO decomposition into atomic N and O on RuO_2(110) has to be attributed to an electronic effect. The existence of electronegative oxygen atoms is expected to decrease the propensity of N−O bond scission by withdrawing electron density from the surface leading to the reduction of electron back-donation into the $2\pi^*$ antibonding orbital of NO. It has been reported that preadsorbed O inhibits NO dissociation

on Ru(0001).[16,21] Actually, the decomposition of NO into atomic N and O has also not been observed on other metal oxide surfaces.

5. Conclusion

The interaction of NO with the $RuO_2(110)$ surface is quite complex and depends on coverage and temperature. Four NO states ($\alpha 1$, $\alpha 2$, β, γ) are observed in TDS and identified from the combined TDS and HREELS results:

(1) The initial exposure (below 0.5 L) of NO at 85 K leads to molecular adsorption of NO-cus which is located on-top of Ru-cus with its molecular axis perpendicular to the surface for the first two-thirds of the monolayer ($\alpha 1$-NO) and slightly bent when the final third of the monolayer ($\alpha 2$-NO) is adsorbed.

(2) At higher exposure an NO_2 surface group is formed through interaction of NO with O-bridge. During annealing to 250 K NO is split-off again (β-NO).

(3) For the whole exposure range, N_2 is formed during an increase of the surface temperature to 190 K and desorbs immediately, as no N_2 is detected in HREELS. The efficiency of the reduction of NO into N_2 is about 25%. It is speculated that N_2 is formed through $(NO)_2$-dimer and N_2O formation, probably at Ru-cus.

(4) At higher exposure, N_2O is formed presumably via an $(NO)_2$ dimer intermediate. A small quantity of N_2O desorbs at about 190 K, giving rise to γ-NO and N_2 as cracking products. The details of N_2O formation are still unclear. Also, the O atom left behind during decomposition of N_2O is not detected.

Acknowledgment. We acknowledge the technical support by P. Geng and the assistance by M. Richard in editing the manuscript and the figures.

References and Notes

(1) Brown, W. A.; King, D. A. *J. Phys. Chem. B* **2000**, *104*, 2578.
(2) Li, G.; Kaneko, K.; Ozeki, S. *Langmuir* **1997**, *13*, 5894.
(3) Wilde, M.; Seiferth, O.; Al-Sharmey, K.; Freund, H.-J. *J. Chem. Phys.* **1999**, *111*, 1158.
(4) Bender, M.; Seiferth, O.; Carley, A. F.; Chambers, A.; Freund, H.-J.; Roberts, M. W. *Surf. Sci.* **2002**, *513*, 221.
(5) Kim, C. M.; Yi, C. W.; Min, B. K.; Santra, A. K.; Goodman, D. W. *Langmuir* **2002**, *18*, 5651.
(6) Over, H.; Kim, Y. D.; Seitsonen, A. P.; Wendt, S.; Lundgren, E.; Schmid, M.; Varga, P.; Morgante, A.; Ertl, G. *Science* **2000**, *287*, 1474.
(7) Wang, J.; Fan, C. Y.; Jacobi, K.; Ertl, G. *Surf. Sci.* **2001**, *481*, 113.
(8) Fan, C. Y.; Wang, J.; Jacobi, K.; Ertl, G. *J. Chem. Phys.* **2001**, *114*, 10058.
(9) Wang, Y.; Lafosse, A.; Jacobi, K. *J. Phys. Chem. B* **2002**, *106*, 5476.
(10) Lafosse, A.; Wang, Y.; Jacobi, K. *J. Chem. Phys.* **2002**, *117*, 2823.
(11) Redhead, P. A. *Vacuum* **1962**, *12*, 203.
(12) Kim, Y. D.; Seitsonen, A. P.; Wendt, S.; Wang, J.; Fan, C.; Jacobi, K.; Over, H.; Ertl, G. *J. Phys. Chem. B* **2001**, *105*, 3752.
(13) Nakamoto, K. *Infrared and Raman Spectra of Inorganic and Coordination Compounds*; Wiley: New York, 1997.
(14) Wang, J.; Fan, C. Y.; Sun, Q.; Reuter, K.; Jacobi, K.; Scheffler, M.; Ertl, G. *Angew. Chem., Int. Ed.* **2003**, *42*, 2151.
(15) Rodríguez-Santiago, L.; Sodupe, M.; Branchadell, V. *J. Phys. Chem. A* **1998**, *102*, 630.
(16) Conrad, H.; Scala, R.; Stenzel, W.; Unwin, R. *Surf. Sci.* **1984**, *145*, 1.
(17) Neyman, K. M.; Rösch, N.; Kostov, K. L.; Jakob, P.; Menzel, D. *J. Chem. Phys.* **1994**, *100*, 2310.
(18) Schmitz, P. J.; Baird, R. J. *J. Phys. Chem. B* **2002**, *106*, 4172.
(19) Nelin, C. J.; Bagus, P. S.; Behm, J.; Brundle, C. R. *Chem. Phys. Lett.* **1984**, *105*, 58.
(20) Dinerman, C. E.; Ewing, G. E. *J. Chem. Phys.* **1970**, *53*, 626.
(21) Jacob, P.; Stichler, M.; Menzel, D. *Surf. Sci.* **1997**, *370*, L185.